NEAR-NUCLEUS IMAGING OF COMET IRAS-ARAKI-ALCOCK 1983H1

D. KUBÁČEK and J. PITTICHOVÁ
Astronomical Institute of the Slovak Academy of Sciences, Dúbravská cesta 9, 842 28 Bratislava, Slovak Republic

Abstract. Several digital image processing techniques were used to improve the visibility of details, fans and jets, in the inner coma of the comet IRAS-Araki-Alcock 1983VII on the short CCD-exposures taken by R. E. Schild with the 61-cm telescope through three I, J, and F band filters, at the Whipple Observatory during the close approach from May 6 through May 12, 1983. About 140 CCD images with the pixel size of 0.73 give a resolution about 20 km, and selected CDD frames presented together with isophotes demonstrate the variation and interrelation of the coma morphology and the nucleus activities during the observing period. Results and processed images are compared with observations taken by other observers during the same period.

Key words: Comet IRAS-Araki-Alcock, near nucleus imaging, computer image processing, coma morphology, near-nucleus jets.

1. Introduction

Comet IRAS-Araki-Alcock 1983H1 (=1983VII) was discovered by the satellite IRAS on April 25, 1983 during the Infrared Sky Survey. The public announcement of the discovery was delayed till May 4, when the comet was discovered independently by two amateur astronomers, G. Araki on May 3.6 UT, and G.E.D. Alcock on May 3.9 UT. The discovery was made only a few weeks before its closest approach to the Earth with the minimal geocentric distance only 0.0313 AU on May 11.5 UT. Such a close approach, the closest one of any comet since comet Lexell in 1770, provided a unique opportunity to observe inner coma and near-nucleus phenomena in great details, and gave us for the first time the chance to try to reveal in radio, IR or optical wavelengths the bare nucleus. Shortly after the discovery it became one of the most studied comets. It was observed almost in all wavelengths from radio to ultraviolet. In addition, the radar observations carried out by Harmon et al. (1989) using the Arecibo 300-m radio telescope, and by Goldstein et al. (1984) using the 64-m antenna at the JPL Goldstone Tracking Station had the aim to get direct measurements of a shape and a size of the comet's nucleus. But the dominant feature of this comet was a fan-shaped coma which is usually observed in some short-period comets, like P/Encke (Djorgovski and Spinrad, 1985), P/Tempel2 (Sekanina, 1987), P/Borrelly and P/Schwassmann-Wachmann 3 (Sekanina, 1979). It is believed that sunward fan comes out of the anisotropic mass ejection from active regions on the cometary nucleus, where comet's spin axis must have a relative small angle to the orbital plane, and the discrete active regions

Earth, Moon and Planets **75:** 1–16, 1997.

should be located near the sunlit rotation pole to be illuminated continuously by the Sun over an extended period of time (Sekanina, 1979, 1987). From the spatial and time variation of the inner coma and near-nucleus phenomena Watanabe (1987) derived rotational parameters of the nucleus of the comet IRAS-Araki-Alcock, and later he reanalysed his data to describe some detailed morphological features of the fan-shaped coma that were neglected in his previous work (Watanabe, 1990). Sekanina (1988) have made probably the most comprehensive analysis of the collected data from various types of detectors and filters covering the broad spectral range, from radio to ultraviolet, and derived with the help of his persistent fan model (Sekanina, 1987) the size and the rotational parameters of the commentary nucleus. Many observations that were carried out during the closest approach gave a spatial resolution close to 20 km (Storrs et al., 1986; Hanner et al., 1985; Jewitt, 1983; Whipple and Schild, 1983; Sykes et al., 1983; Barker and Cochran, 1983; Storrs et al., 1983). Images presented in this paper were kindly provided by R. E. Schild, and represent only a small part of selected short CCD-exposures that have been used to test some digital image processing techniques suitable for the study of the spatial and time variation of the inner coma and near-nucleus phenomena.

2. Observations, Data Reduction, and Image Processing

As was mentioned above, the observations were obtained by R.E. Schild (Whipple and Schild, 1983; Sykes et al., 1983) with the RCA CCD camera at the f13.5 Cassegrain focus of the Whipple Observatory 61-cm telescope during the nights from May 6 till May 12, 1983. This configuration provided a scale of 0.73 arcsec/pixel, and for the whole chip of the 320 × 512 pixel image the field of view reached of the 3.9 × 6.2 arcmin in size. All CCD images were taken through three broad band filters: the J band filter covers the spectral range of the 390–550 nm; the F and I filters are a little overlaping and span the spectral regions of the 570–770 nm and 770–900 nm, respectively. Each of the bands is approximately 150 nm wide at half maximum transmission. Data were reduced by standard techniques by the observer at the CfA. A zero exposure data frame, the mean of several frames taken through the each night, was subtracted and the corrected data frame was flat field-corrected with flat field frames exposed to a white painted spot on the surface of the closed telescope dome. In addition, the images were cleaned for hot spots and for defective columns by interpolation across the nearest adjacent columns. From the whole set of about 140 CCD images we picked up 56 frames taken on May 10, 1983. All the necessary information about the comet and CCD images are listed in Table I. Because of a rapid motion of the object, the image of the comet did not always fall on the same region of the chip and in many cases not whole fan coma was recorded. For our purposes to study mainly near-nucles phenomena we clipped the image patches to the 256 × 256 pixel size or for faster calculations only to the size of 128 × 128 pixels. The optocenter of the comet had been placed

Table I

CCD	t 1983 (UT)	R.A.	DEC	r	d	exp.	Flt
No.	m d	h m s	o ′ ″	AU	AU	s	
15965	05 10.00438	15 14 10	+73 35 16	1.00997	0.04903	10	J
15967	05 10.00625	15 13 41	+73 35 41	1.00996	0.04899	1	F
15968	05 10.01041	15 12 36	+73 36 36	1.00995	0.04891	20	F
15969	05 10.01285	15 11 57	+73 37 08	1.00994	0.04886	1	F
15970	05 10.01323	15 11 51	+73 37 13	1.00994	0.04885	2	F
15971	05 10.01681	15 10 54	+73 37 60	1.00993	0.04878	20	F
15972	05 10.02424	15 08 56	+73 39 33	1.00990	0.04864	20	F
15973	05 10.03147	15 06 60	+73 41 00	1.00988	0.04850	30	F
15974	05 10.03274	15 06 39	+73 41 15	1.00988	0.04848	30	I
15975	05 10.03389	15 06 21	+73 41 28	1.00987	0.04845	30	J
15977	05 10.04069	15 04 30	+73 42 46	1.00985	0.04832	30	J
15978	05 10.04171	15 04 14	+73 42 58	1.00985	0.04830	30	I
15979	05 10.04267	15 03 58	+73 43 08	1.00984	0.04828	30	F
15981	05 10.04957	15 02 04	+73 44 23	1.00982	0.04815	30	F
15982	05 10.05058	15 01 48	+73 44 34	1.00982	0.04813	30	I
15983	05 10.05172	15 01 29	+73 44 46	1.00981	0.04811	30	J
15985	05 10.05980	14 59 15	+73 46 07	1.00979	0.04795	3	J
15986	05 10.06168	14 58 43	+73 46 26	1.00978	0.04792	3	J
15987	05 10.06360	14 58 11	+73 46 44	1.00977	0.04788	3	J
15989	05 10.07571	14 54 47	+73 48 34	1.00974	0.04765	30	J
15990	05 10.07705	14 54 24	+73 48 46	1.00973	0.04762	30	F
15991	05 10.07834	14 54 02	+73 48 57	1.00973	0.04760	30	I
15996	05 10.09773	14 48 28	+73 51 25	1.00966	0.04723	1	F
15997	05 10.09850	14 48 15	+73 51 31	1.00966	0.04722	1	F
15998	05 10.09891	14 48 08	+73 51 34	1.00966	0.04721	1	F
15999	05 10.09933	14 48 00	+73 51 36	1.00966	0.04720	1	F
16000	05 10.09975	14 47 53	+73 51 39	1.00966	0.04719	1	F
16001	05 10.10019	14 47 45	+73 51 42	1.00966	0.04718	1	F
16002	05 10.10061	14 47 38	+73 51 45	1.00965	0.04718	1	F
16003	05 10.11747	14 42 42	+73 53 25	1.00960	0.04686	1	F
16004	05 10.11786	14 42 35	+73 53 27	1.00960	0.04685	1	F
16005	05 10.11824	14 42 28	+73 53 29	1.00960	0.04684	1	F
16006	05 10.11876	14 42 19	+73 53 31	1.00960	0.04683	1	F
16007	05 10.11919	14 42 11	+73 53 34	1.00959	0.04682	1	F
16008	05 10.11985	14 41 59	+73 53 37	1.00959	0.04681	1	F
16009	05 10.12029	14 41 52	+73 53 39	1.00959	0.04680	1	F
16047	05 10.91781	10 44 40	+63 09 10	1.00710	0.03449	30	F
16048	05 10.92194	10 43 49	+63 01 43	1.00708	0.03444	3	F
16049	05 10.92248	10 43 42	+63 00 44	1.00708	0.03444	3	F
16050	05 10.92798	10 42 35	+62 50 45	1.00707	0.03438	30	F
16051	05 10.93051	10 42 04	+62 46 09	1.00706	0.03435	30	F
16052	05 10.93272	10 41 37	+62 42 06	1.00705	0.03433	30	I
16054	05 10.93524	10 41 07	+62 37 28	1.00704	0.03430	30	I
16055	05 10.93693	10 40 47	+62 34 22	1.00704	0.03428	30	I
16056	05 10.93854	10 40 28	+62 31 24	1.00703	0.03427	30	J
16057	05 10.94053	10 40 04	+62 27 43	1.00703	0.03425	30	J
16058	05 10.94190	10 39 47	+62 25 11	1.00702	0.03423	30	J

Table I
Continued

CCD No.	t 1983 (UT) m d	R.A. h m s	DEC ° ′ ″	r AU	d AU	exp. s	Flt
16059	05 10.94404	10 39 22	+62 21 13	1.00702	0.03421	60	J
16060	05 10.94610	10 38 57	+62 17 23	1.00701	0.03419	60	F
16062	05 10.94983	10 38 13	+62 10 25	1.00700	0.03415	60	I
16063	05 10.95154	10 37 53	+62 07 13	1.00699	0.03413	60	F
16065	05 10.95324	10 37 33	+62 04 02	1.00699	0.03411	60	J
16068	05 10.96969	10 34 22	+61 32 52	1.00694	0.03395	60	J
16070	05 10.97178	10 33 58	+61 28 52	1.00693	0.03393	60	F
16072	05 10.97427	10 33 30	+61 24 05	1.00693	0.03390	60	I

into the lower left corner of the patches to get the fan as large as possible into the clipped frame. The observer claims, according to the FITS header, that the seeing during the observations on May 10 varied from 1.0″ to 1.5″, but according to our measurements the FWHM of several selected stars from one second exposures varied in a range of 1.8″ to 2.5″, with the mean about of 2.2 arcsec. Except of 1, 2, and 3-second exposures all others, 10, 20, 30, and 60-second frames were guided to follow the comet motion. In all image processing techniques which we have employed, the background, where it was necessary, was calculated in small boxes located in the regions without the source, usually close to the edges of the frames, or in smaller images we figured out the mean value of the coma in those boxes, and average value was considered as sky background. There are several review articles dealing with the image processing techniques applied in cometary imaging (Matuska et al., 1978; Klinglesmith, 1981; Larson, 1986; A'Hearn et al., 1986; Schwarz et al., 1989; Larson and Slaughter, 1992), and in our tests we tried several of them to get more information about the structures in the inner part of fan-shaped coma. It should be noted that we did not apply any processing on the 1, 2, and 3-second exposures, and we only co-added these images to reduce the noise to make visible the fan. For all employed image processing techniques we picked up the frame No 16051 (see Table I) and then we chose the only one method to process all time sequence of images of May 10.

The first, we applied some digital filters, like a digital sharpening or unsharp masking, a directional gradient filtering, an offset masking, and some others, but these simple digital filters, usually represented by a convolution of the original image with small kernels, did not work well for this type of data, where a very low contrast fan-shaped coma is superimposed on the bright central condensation with a very steep intensity gradient. Almost in all cases the fan was completely removed, and the central condensation was too noisy to see any clear structure. Similarly we did not get very good results with the general unsharp masking (Malin, 1977; Matuska et al., 1978; Larson, 1985) where a low pass filtered version of an image is subtracted from the original image. Klinglesmith (1981) described

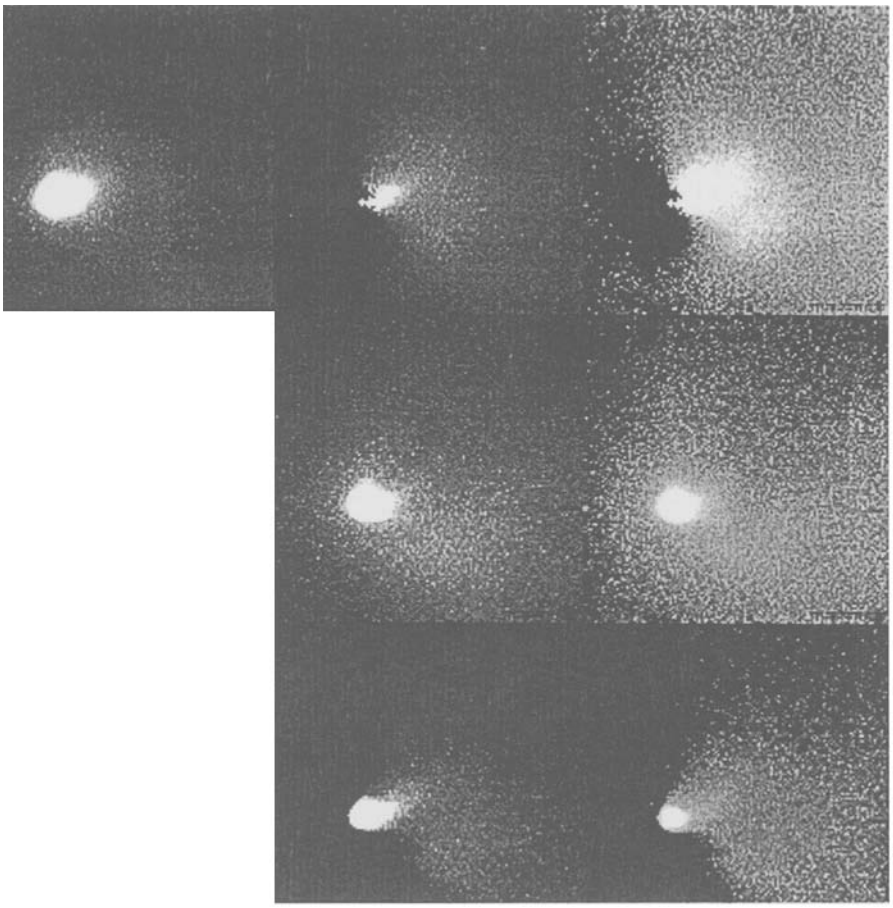

Figure 1. The comparison of three methods that enhance different features in the inner fan coma. All displayed images have the size of 128 × 128 pixels.
The first row from left to the right:
– Unprocessed image CCD No 16051.
– The inner coma was unmasked with the azimuthal renormalization. The broad fan and sunward-curved jet are clearly visible. The sharp cut in the northern part of the fan coma corresponds with the position of the faint, narrow jet emanating from the nucleus towards the North. The image is displayed in a linear scale.
– The same image but displayed in a logarithmic scale to bring some information from more distant part of the coma.
The second row:
– The coma was unmasked with the synthetic image based on a generalized model of particle outflow. Such model has been created by median of 30-sec. exposures. The straight, faint jet directed to the North, central curved outflow, and some southern asymmetry in the fan are more legible. Both images are displayed in the same way as in the first row.
The third row:
– The central sunward jet and south-west broad outflow are enhanced with the help of the mask in which the intensity distribution follows the $1/r$ law. Left image is displayed in linear and right one in logarithmic scale.

Table II

CCD No.	FnSp [']	p.a. [o]	NSJ ["]	SCJ ["]	S-WBO ["]	Note
15965	1.0	305				1,4
15968	2.4	312				4
15971	1.4	309				1,4
15972	2.1	308				4
15973	2.8	309				4
15974	3.0	309				4
15975	2.7	309				4
15977	2.9	310				4
15978	2.3	309				4
15979	2.6	306				4
15981	2.6	306				4
15982	2.1	305				4
15983	2.6	305				4
15989	3.2	304				4
15990	2.1	305				4
15991	1.9	305				4
16047	3.0	281	57	35	31	
16050	2.7	271	54	14	47	
16051	3.2	273	84	22	24	
16052	3.4	273	72	22	34	
16054	2.8	274	72	17	23	
16055	2.7	270	53	20		5
16056	2.0	270	44	13		5
16057	2.3	270	49	14		5
16058	1.9	274	60	24	33	
16059	3.0	270	59	30	37	
16060	4.8	270	96	26	39	2
16062	3.4	270	78	24	37	1
16063	5.2	270	90	35	41	2
16065	4.9	270	72	26	41	
16068	4.8	271	56	25	42	
16070	3.8	276		34	49	1,3
16072	3.9	275		30	34	1,3

FnSp ['] – the estimate of the maximum span of the coma in direction of p.a.

p.a. [o] – the position angle of the direction of the maximum span of coma. Angles are counted in the counterclockwise direction from the North through the East.

NSJ ["] – the estimate of the length of the Northern Straight Jet.

SCJ ["] – the estimate of the length of the Sunward Curved Jet.

S-WBO ["] – the estimate of the length of the South-West Broader Outflow.

1 – The comet is close to the edge of the chip.

2 – The coma of the comet fills up almost whole chip.

3 – NSJ visible but not measured due to 1.

4 – SCJ detected but not measured.

5 – W-SBO was very faint, not measured.

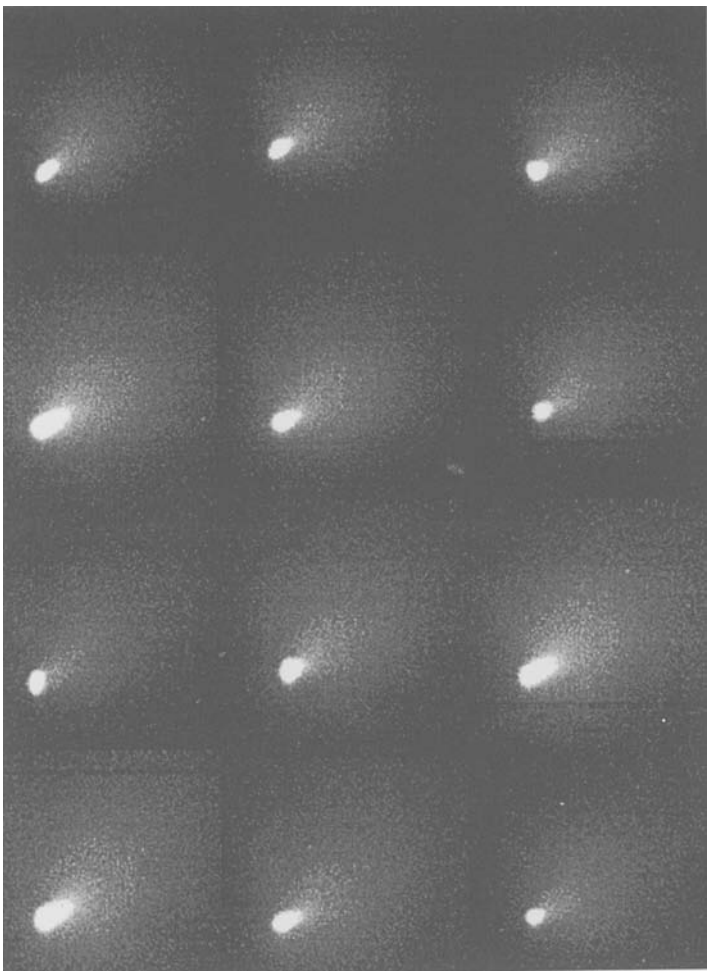

Figure 2. The space/time and shape variation of the inner fan coma of the comet IRAS-Araki-Alcock on May 10, 1983.

gradient/masking method, so called "shift-difference" techinque which emphasizes edges of intensity boundaries. Later Larson and Sekanina (1984) improved this algorithm and they developed the radial and rotational shift-difference method in response to the fact that particles usually escape from the cometary nucleus in the radial direction, and that the rotating nucleus can produce spiral features (for good example see also: Sekanina, 1991). We tried the both methods, but without any great success. The explanation gives the Sekanina's fan-model itself, in which the rotating nucleus with active areas close to the sunlit rotating pole cannot create large spiral features in surrounding coma, as it was observed in the case of the comet P/Halley (Larson and Sekanina, 1984, 1985; Sekanina and Larson, 1984,

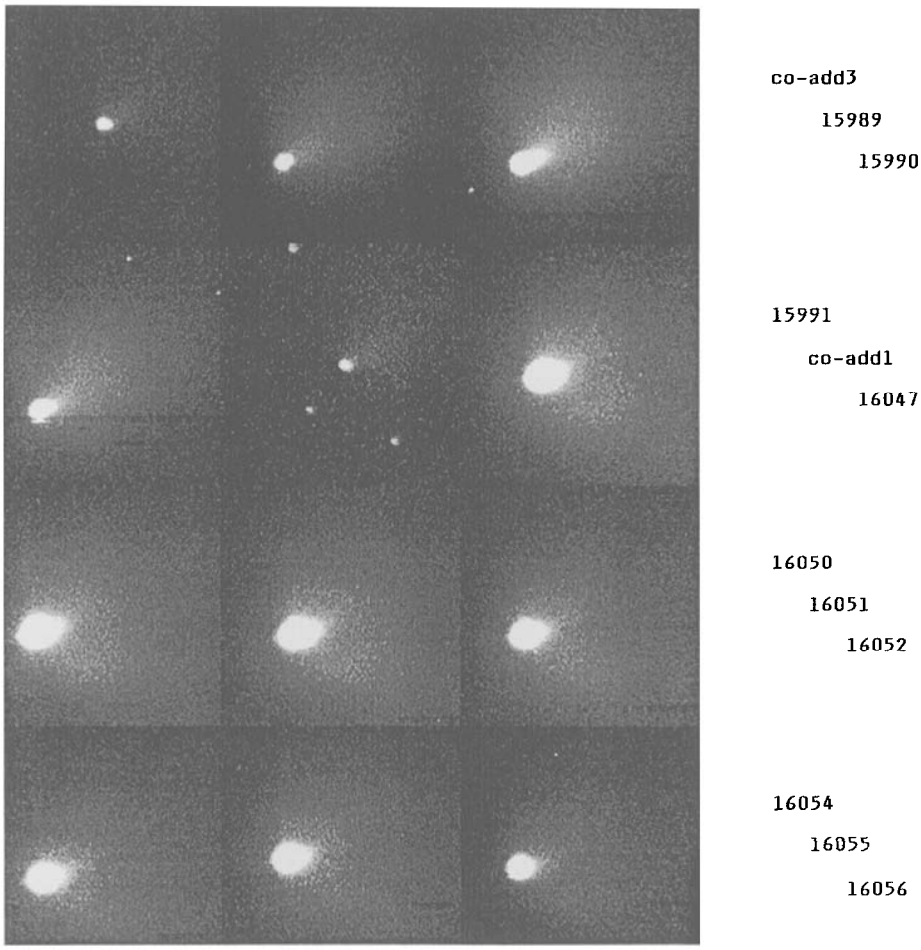

Figure 2b.

1986). We found that the algorithm which is fitting best to our data is based on the azimuthal renormalization. It was invented by A'Hearn et al. (1986) for their study of the CN emission of the comet P/Halley. This method reduces the radial gradient of the coma and enhances its faint, low contrast features. The resulting image is so called net image of the coma (Boehnhardt, 1992). Our implementation of this algorithm is similar to the Larson's one (Larson and Slaughter, 1992), without a polar/rectangular coordinate conversion. In all images that we have processed with this method the fan-shaped coma is clearly enhanced, and in the region close to the nucleus there are some indications of curved jet-like structure extended into the sunward inner coma. Another type of a similar algorithm utilizes a simplified isotropic model of a coma in which the surface brightness distribution follows the

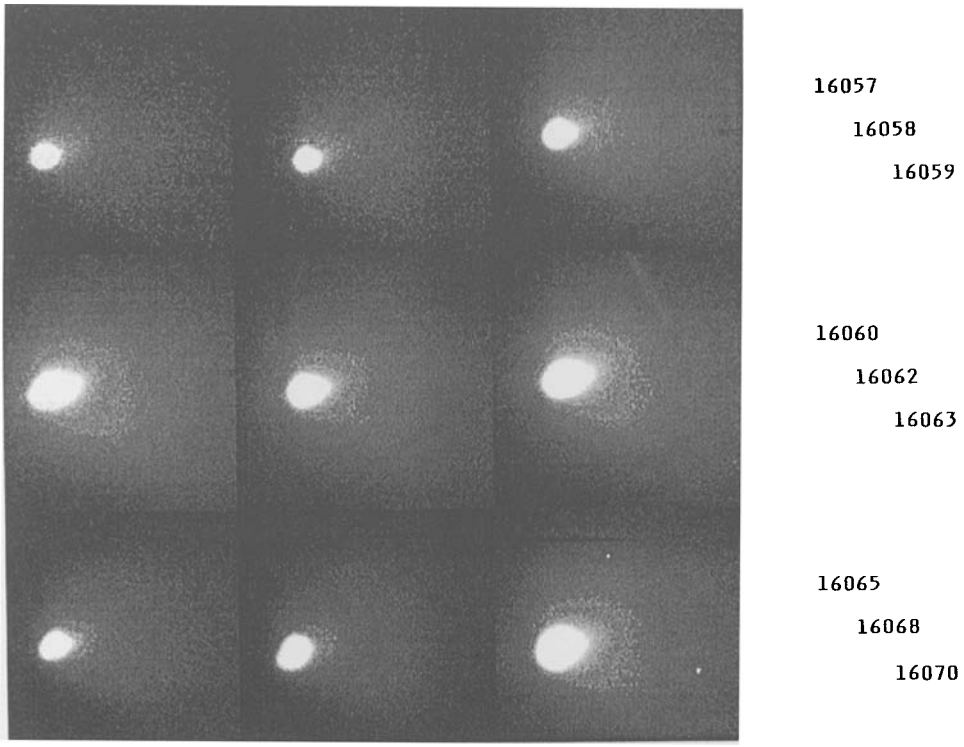

Figure 2c.

$1/r$ law, where "r" is the projected distance to the nucleus. To enhance anisotropic low contrast features which are superimposed on the $1/r$ intensity gradient of the surrounding coma, one can subtract the ideal $1/r$ model of the coma convolved with a Gaussian of the FWHM of a seeing to get more real coma, in which the intensity distribution can be normalized in that way that it will match the intensity in a real coma in particular directions. In our case, after the background subtraction, we simply normalized the total flux of a model to the the total flux of the comet. The result image shows that in a fan-shaped coma there exists an anisotropic outflow of particles. Another similar approach that we have also employed was proposed by Jewitt (1991). He proposed to subtract a synthetic image based on generalized model of particle outflow. To create such a model some *a priori* knowledge of the ejection function is assumed, or if there is enough data a model/mask can be created by the median of many images. We have used 21 images to create the mask for 30-second exposures, and this mask was subtracted from the individual frames after a renormalization to the total flux of individual images. In our pictures this method enhanced the straight faint jet which escapes from the nucleus to the north, and reaches the length on the best images of about $1.5'$. The results of the last three methods mentioned above are shown in Figure 1. As the final step in our image

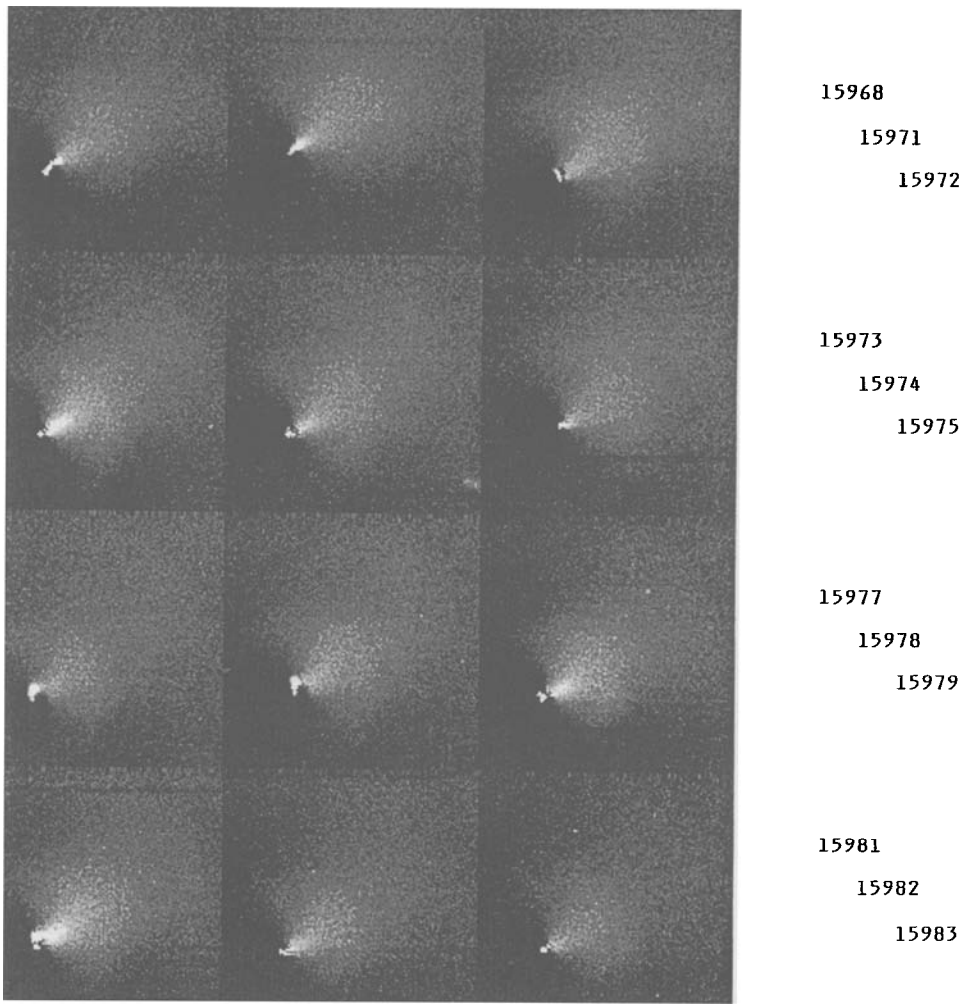

Figure 3. The same set of images as in Figure 2, but processed with azimuthal renormalization. Some artifacts visible at the origin of the fan are mainly due to the rapid motion of the comet and its unperfect guiding, or defective pixels, but the curved sunward outflow is apparent in all images, even in 1 and 3-sec. co-added frames.

processing we tried to deconvolve image of the comet IRAS-Araki-Alcock with the maximum likelihood algorithm proposed by Richardson (1972) and Lucy (1974). The point spread function was created from selected stars by fitting a Gaussian functional form to the averaged star. But as the deconvolution was doing progress towards to the sharp central condensation, the outer part of coma was becoming more and more noisy. We decided to stop this process, and we concluded that for our images will probably be more suitable a new version of this algorithm improved by Hook and Lucy (1992, 1993), and Hook et al. (1994).

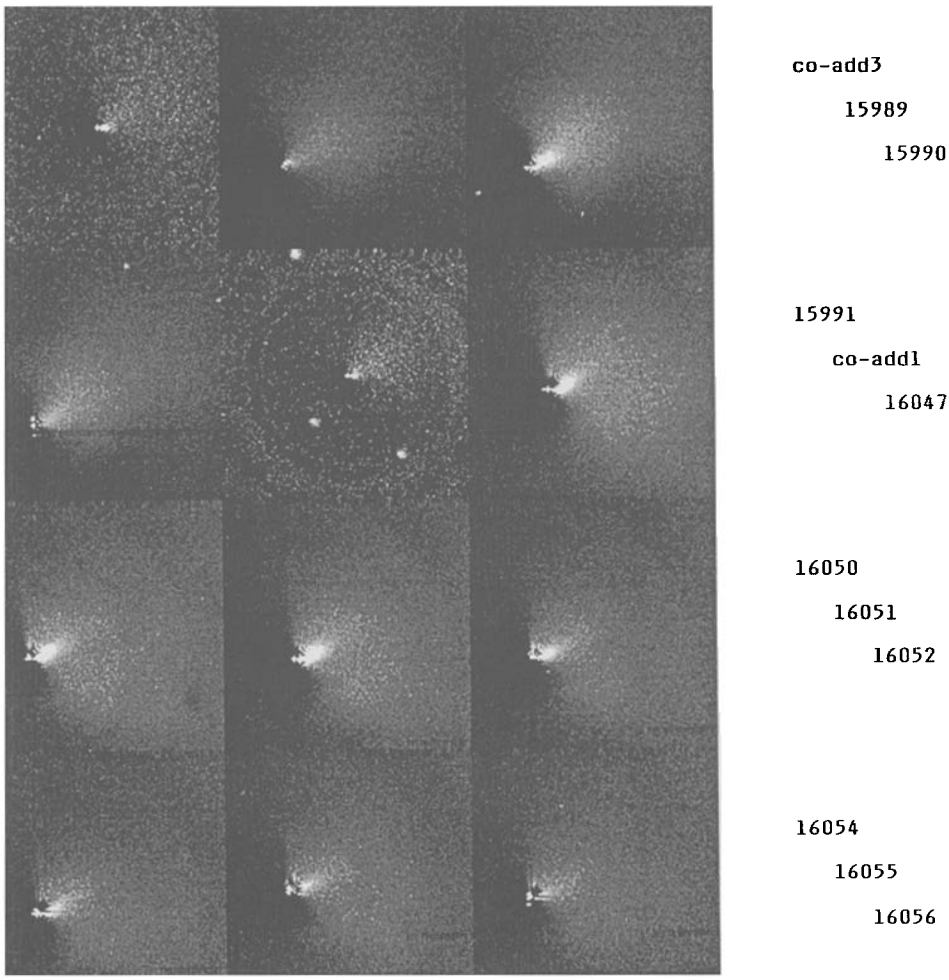

Figure 3b.

3. Coma Morphology and Near-Nucleus Jets

General feature of the gas/dust outflows from the nucleus of comet IRAS-Araki-Alcock, fan-shaped coma is clearly visible in all presented images, in both types of data, unprocessed and processed, too (Figures 2 and 3). The size, shape, and structures observed in fan depend on time of integration and on instantaneous observing conditions, but at the first glance one can see that sunward fan and coma as a whole are fainter and less evolved in the first half of the set of displayed images, CCD No. 15968–CCD No. 15991, than in all other images which were exposed about 19 hours later. The fan in these images (15968–15991) looks symmetric around the axis which deviates from the direction of the apparent position of

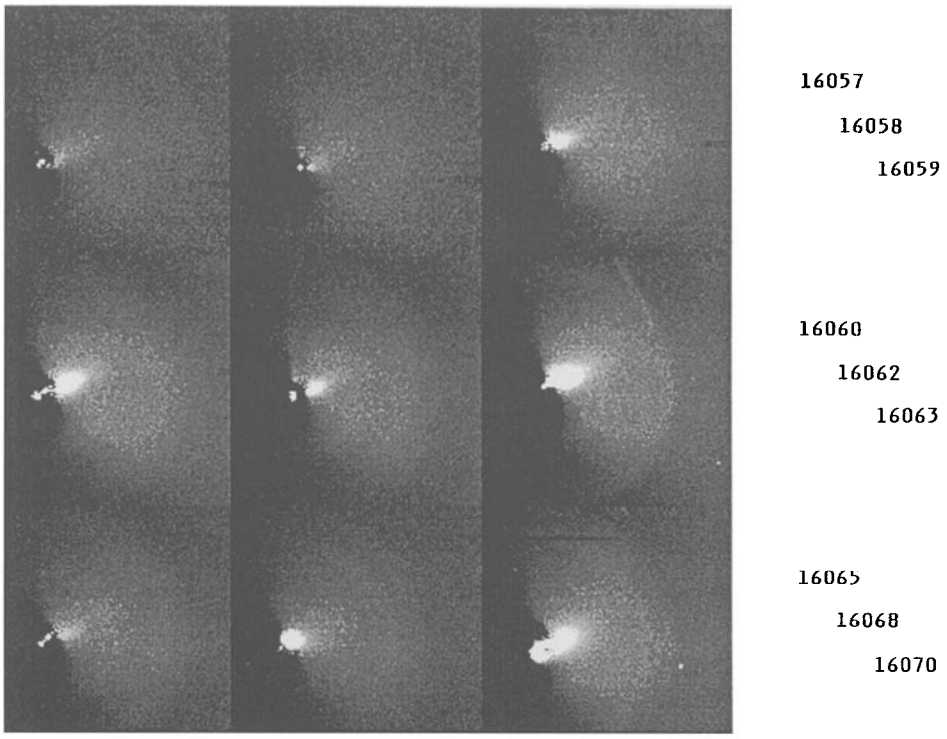

Figure 3c.

the Sun on the sphere only about 10° to south. It should be noted that all 30 and 60-second exposures were equally scaled to get relatively the same intensity distribution in displayed images. Better evolved coma with some internal structures is present in the second half of the set of images of May 10. The distinct features that can be revealed in the coma of a comet are shown in Figure 1. In the first upper row, the image on the left is an unprocessed image of the CCD frame No. 16051, the next one to the right is the same image processed with an azimuthal renormalization technique and shows a clear fan-shaped coma and a central sunward curved jet (SCJ). The last image of the first row is the same one, but displayed in a logarithmic scale to see also the outer part of a fan-coma. In the second row the same raw data are processed with some kind of unsharp masking, where the mask subtracted from the original image was created from 21 frames of 30-second exposures. These images, the first displayed in a linear and the second one in a logarithmic scale, enhance the straight narrow jet directed to the north, the central asymmetry of the innermost coma which can be identified with the SCJ, and some southern outflow asymmetry which is more legible in the third row. Images in the third row, displayed in the same way as the previous ones were processed with the mask in which the intensity distribution follows $1/r$ law. This south-west broad

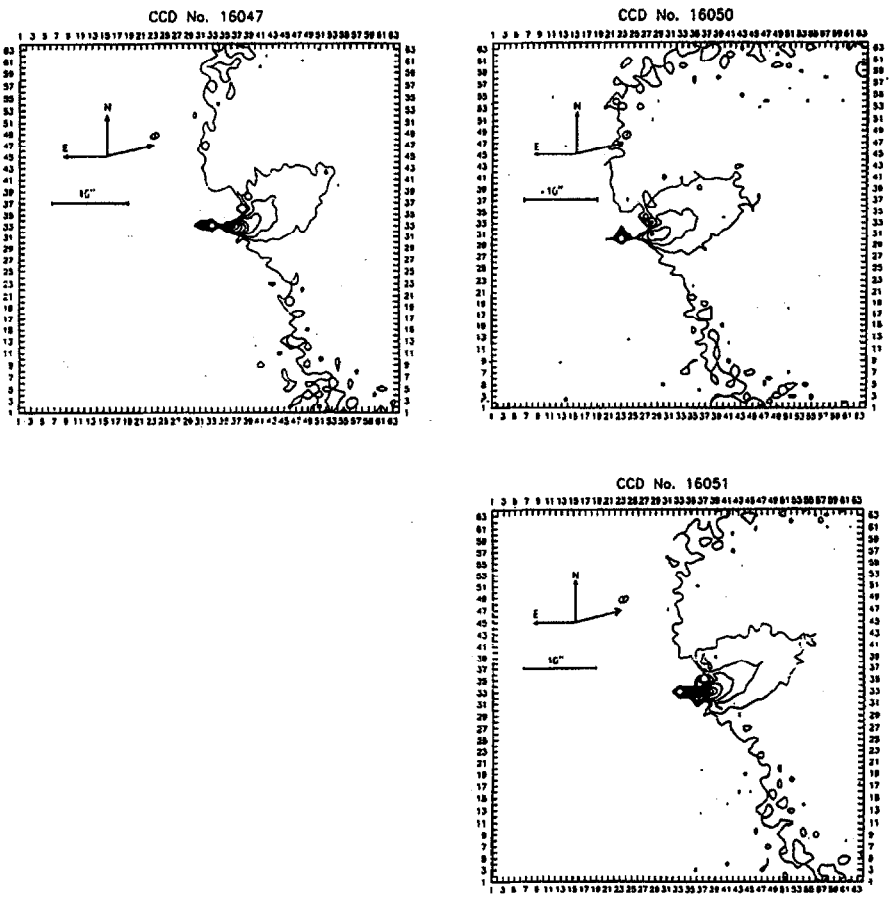

Figure 4. The contour plots of the innermost part of the coma to show the detailed structure of the best defined sunward curved jets in images processed with azimuthal renormalization. Contours at intervals of 50, starting at 20, peak at 4000.

outflow (S-WBO) asymmetry is prominent in the second half of the set of images of May 10; CCD frames No. 16047–CCD No. 16072. The SCJs are also detected in the first half of the set (15968–15991), but are not so prominent as in the second one. These features are better seen in the contour plots of the innermost part of the coma of a size 64 pixels square. If one is playing interactively only with the intensity transform table, the northern straight jet (NSJ) is clearly visible in all frames from CCD No. 16047, and on the best exposures it reaches the length up to 1.5′ which corresponds to the distance of about 2200 km far from the nucleus. The inner fan-coma in these unprocessed images looks like a trident with three distinct jets or broader outflows, similarly as in Figure 1 in Hanner et al. (1985). Therefore it is possible that a fan is composed of a few diffuse jets, and that the observations at high resolution, which could be our case, may separate these jets near their source

(Keller et al., 1987). The coma in the second half of the set was elongated mainly towards the west with definite asymmetry to the south, and on the best exposures it filled up almost the whole CCD chip. The space and time variations in the fan and near-nucleus jets can be visible in Figures 2 and 3. In all images the North is up and East is to the left. The left image in the fifth row of the Figure 2 is a co-added image of 3-second exposures, CCD frames No. 15985, 15986, and 15987, and the second one in the sixth row is co-added image created from 8, one-second CCD frames exposed between May 10.98 UT and May 10.12 UT. In the both co-added images the sunward fan is clearly visible, too. The sunward curved jet which is really present in all images of Figure 3a,b,c has the best defined shape on the frames No. 15990, 16047, 16050, 16051, 16052, 16054, and 16058, which is also demonstrated in contour plots in Figure 4. This sunward curved jet originated from nucleus at the position angle about 270° or a little less, and turned towards the Sun, to the position angle of about 305° to 310° during its expansion into the surrounding coma. The presence of jets, a straight narrow jet, a sunward curved jet, and a broader outflow in the inner coma can be interpreted due to at least three isolated active regions on rotating nucleus as proposed by Sekanina (1988) in his model of a nucleus of the comet IRAS-Araki-Alcock. Some quantitative estimates of structures in the fan-shaped coma are listed in Table II. We did not make any detailed analysis of the sunward curved jet, it will be given elsewhere, but according to its shape, and under the assumption that S-WBO could be a diffuse tail of a jet which originates in the active region placed on the opposite, invisible, sunlit hemisphere, the sense of rotation seems to be inconsistent with the one accepted by Sekanina (1988).

4. Conclusions

We found that for our purposes to study near-nucleus phenomena in the comet IRAS-Araki-Alcock, the azimuthal renormalization have provided the best results and clearly revealed internal structures in the fan-shaped coma that can be used in the further analyses for determination of the rotational parameters of the nucleus of this comet. The advantage of this method is that it gives the straightforward interpretation of the processed images. The artifacts that can be seen in the central part of the innermost coma are mainly due to the rapid motion of the comet and its inperfect guiding. Because every masking process brings up into the processed image more noise, some improvements of the azimuthal renormalization can be made with options for averaging over various ranges of radius and azimuth. In our implementation these improvements are in a progress. As was mentioned above, we would like to try for this data the so-called multichannel deconvolution either in the maximum likelihood process (Hook et al., 1994) or in the maximum entropy one (Weir, 1991).

A preliminary analysis of the series of CCD images of the comet IRAS-Araki-Alcock showed that fan-shaped coma contains some internal structures which can

be identified with asymmetric gas/dust outflows from active regions on rotating nucleus. Processed images confirmed the correctness of a fan model of coma proposed by Sekanina (1987). Comparing all images is evident that on May 10.9 UT began a sudden activity on cometary nucleus which can be observed as the jets, NSJ and SCJ, and S-WBO. The persistence of these features during rotating nucleus. Processed images confirmed the correctness of a fan model of coma proposed by Sekanina (1987). Comparing all images is evident that on May 10.9 UT began a sudden activity on cometary nucleus which can be observed as the jets, NSJ and SCJ, and S-WBO. The persistence of these features during all observations on May 10 indicates that the rotation period could correspond to the one proposed by Sekanina (1988), but the shape of the innermost jet and fan coma asymmetry show that sense of rotation accepted by Sekanina (1988) seems to be ambiguous.

Acknowledgements

The authors are grateful to Rudolph E. Schild who kindly provided his whole set of CCD images for our test and further analysis. We also wish to thank Barnabaš Mišánik for his help in printing the compressed version of postcript images; Figures 1, 2, and 3. This work was supported by the Slovak Academy of Sciences VEGA Grant No. 1050/1966.

References

A'Hearn, M. A. F., Hoban, S., Birch, P. V., Bowers, C., Martin, R., and Klinglesmith III, D. A.: 1986, *Nature* **324**, 649–651.

Barker, E. S. and Cochran, A. L.: 1983, *Bull. Am. Astron. Soc.* **15**, 800–806.

Boehnhardt, H., Vanýsek, V., Birkle, K., and Hopp, U.: 1992, in A. W. Harris and E. Bowell (eds.), *Asteroids, Comets, Meteors 1991*, Lunar and Planetary Institute, Houston, pp. 81–84.

Djorgovski, S. and Spinrad, H.: 1985, *Astron. J.* **90**, 869–876.

Goldstein, R. M., Jurgens, R. F., and Sekanina, Z.: 1984, *Astron. J.* **89**, 1745–1754.

Hanner, M. S., Aitken, D. K., Knacke, R., McCorkle, S., Ropche, P. F., and Tokunaga, A. T.: 1985, *Icarus* **62**, 97–109.

Harmon, J. K., Campbell, D. B., Hine, A. A., Shapiro, I. I., and Marsden, B. G.: 1989, *Astrophys. J.* **338**, 1071–1083.

Hook, R. and Lucy, L. B.: 1992, *ST-ECF Newsletter* **17**, 10–11.

Hook, R. and Lucy, L. B.: 1993, *ST-ECF Newsletter* **19**, 6–7.

Hook, R., Lucy, L. B., Stockton, A., and Ridgway, S.: 1994, *ST-ECF Newsletter* **21**, 16.

Jewitt, D.: 1983, *Bull. Am. Astron. Soc.* **15**, 799.

Jewitt, D.: 1991, in R. L. Newburn Jr., M. Neugebauer, and J. Rahe (eds.), *Comets in the Post-Halley Era*, Vol. 1, Kluwer Academic Publishers, Dordrecht, pp. 19–65.

Keller, H. U., Delanere, W. A., and Huebner, W. F. et al.: 1987, *Astron. Astrophys.* **187**, 807–823.

Klinglesmith III, D. A.: 1981, in J. C. Brandt, B. Donn, J. M. Greenberg, and J. Rahe (eds.), *Modern Observational Techniques for Comets*, JPL Publication 81-68, Pasadena, pp. 223–231.

Larson, S. M.: 1986, in C.-I. Lagerkvist, B. A. Lindblad, H. Lundstedt, and H. Rickman (eds.), *Asteroids, Comets, Meteors II*, Uppsala Universitet, Uppsala, pp. 449–459.

Larson, S. M. and Sekanina, Z.: 1984, *Astron. J.* **89**, 571–606.

Larson, S. M. and Sekanina, Z.: 1985, *Astron. J.* **90**, 823–826.

Larson, S. M. and Slaughter, C. D.: 1992, in A. W. Harris and E. Bowell (eds.), *Asteroids, Comets, Meteors 1991*, Lunar and Planetary Institute, Houston, pp. 337–343.
Lucy, L. B.: 1974, *Astron. J.* **79**, 745–754.
Malin, D. F.: 1977, *AAS Photo-Bulletin* **16**, 10–11.
Matuska, W., Janney, D. H., Farrell, J. A., and Keller, C. F.: 1978, *Optical Engineering* **17**, 661–665.
Richardson, W. H.: 1972, *Journal of the Optical Society of America* **62**, 55–63.
Sekanina, Z.: 1979, *Icarus* **37**, 420–442.
Sekanina, Z. and Larson, S. M.: 1984, *Astron. J.* **89**, 1408–1447.
Sekanina, Z. and Larson, S. M.: 1986, *Astron. J.* **92**, 462–482.
Sekanina, Z.: 1987, in E. J. Rolfe and B. Battrick (eds.), *Diversity and Similarity of Comets*, ESTEC ESA SP-278, Noordwijk, pp. 315–322.
Sekanina, Z.: 1988, *Astron. J.* **95**, 1876–1894.
Sekanina, Z.: 1991, in R. L. Newburn Jr., M. Neugebauer, and J. Rahe (eds.), *Comets in the Post-Halley Era*, Vol. 2, Kluwer Academic Publishers, Dordrecht, pp. 769–823.
Schwarz, G., Cosmovici, C., Mack, P., and Ip, W.: 1989, *Adv. Space Res.* **9**, 217–220.
Storrs, A. D. and Tokunaga, A. T., Heasley, J. N., and Christian, C. A.: 1983, *Bull. Am. Astron. Soc.* **15**, 801.
Storrs, A. D., Tokunaga, A., Christian, C. A., and Heasley, J. N.: 1986, *Icarus* **66**, 143–153.
Sykes, M. V., Larson, S. M., Schneider, N. M., Hunten, D. M., and Schild, R. E.: 1983, *Bull. Am. Astron. Soc.* **15**, 800.
Watanabe, J.: 1987, *Pub. Astron. Soc. Japan* **39**, 485–503.
Watanabe, J.: 1990, *Publ. Natl. Astron. Obs. Japan* **4**, 331–342.
Weir, N.: 1991, in P. J. Grosbol and R. H. Warmels (eds.), *3rd ESO/ST-ECF Data Analysis Workshop*, ESO, Garching, pp. 115–121.
Whipple, F. L. and Schild, R. E.: 1983, *Bull. Am. Astron. Soc.* **15**, 799–800.